Quadrature polarimetry for plasma Faraday rotation measurements

John Howard
Plasma Research Laboratory, Research School of Physical Sciences and Engineering, Australian National University, Canberra, A.C.T., Australia

(Presented on 9 May 1994)

A quadrature polarimeter for measurement of plasma magnetic field and electron densities is described. The polarization ellipse tilt angle is encoded as a relative phase shift between orthogonally polarized beams. This phase can be recovered using standard quadrature interferometric methods. The results from a benchtop experiment are presented. © *1995 American Institute of Physics.*

I. INTRODUCTION

The change of polarization of a probing laser beam traversing a magnetized plasma is a useful electron density or internal magnetic field diagnostic.[1–3] The Faraday rotation angle of the electric vector is given by[4]

$$\psi \approx 2.6\times 10^{-13}\lambda_0^2\int_0^L n_e B_\parallel \, dl. \tag{1}$$

where λ_0 is the laser vacuum wavelength (typically infrared to far-infrared) and $B_\parallel = \mathbf{B}\cdot\widehat{d\mathbf{l}}$, where $\mathbf{B}$ is the magnetic field, $\widehat{d\mathbf{l}}$ is the unit vector in the propagation direction, n_e is the electron density, dl is a line element, and SI units are used. Usually, n_e is determined by measuring interferometrically the refractive phase shift φ,[4] allowing $B_\parallel$ to be inferred from measurements of ψ at a sufficient number of positions. Measurement of ψ may also be a useful density diagnostic when $B_\parallel$ is known.[3,5]

Recently, a new type of spatially scanning phase-sensitive heterodyne interfero-polarimeter has been proposed for simultaneous measurement of the refractive phase shift φ and the Faraday rotation angle ψ.[6] The latter is encoded as a differential phase shift between intermediate frequency signals obtained at two detectors sensing orthogonal polarization components of the probe beam. The interferometric phase is common to both beams.

It is usually the case, however, that the plasma Faraday rotation is small enough that $\sin\psi = \psi$ to sufficient accuracy. Sophisticated frequency-shifted heterodyne methods for phase-shift measurements may not then be warranted. Without the frequency offset, however, sensitivity to φ as in the case of the interfero-polarimeter described above would confuse the measurement of ψ. It is thus desirable to obtain a measurement of ψ independent of φ. This might also considerably relax the experimental burden, in that elaborate arrangements for vibration suppression are not necessary for removal of phase noise due to path length variations.

The simplest polarimetric scheme is to measure the intensity of the rotated electric field component through an analyzer oriented to reject the unperturbed probe beam.[7] The transmitted component is usually mixed with an independent, frequency offset local oscillator and the amplitude of the resulting beat signal is proportional to ψ. Various other beam mixing methods have also been tried.[8–11] We describe here a polarimeter that is sensitive to the quadrature and in-phase components of the polarization angle modulation ψ. The method is insensitive to laser power variations and path length changes in the probe beam optical circuit and is robust to plasma refractive beam bending. Using a local oscillator derived from the Faraday rotated beam itself, the signals obtained at the two output ports can also be made proportional to $\pm 2\psi$.

The polarimeter is to be installed for density measurements in the H-1 heliac at the Australian National University.[12] MHD computations suggest that the instrument should serve well as a routine densitometer for the initially low beta, ion-cyclotron heated plasmas.[3] The principle of the polarimeter is discussed using the Jones matrix formalism in Sec. II. Finally, results for a millimeter wave polarimeter designed to check the theory are described in Sec. III.

II. PRINCIPLE

We allow the plasma to be both optically active and linearly birefringent so that the modified polarization state can be represented as the complex vector

$$\mathbf{E} = \begin{pmatrix} \cos\eta \\ \sin\eta \exp j\phi \end{pmatrix}, \tag{2}$$

where $\tan\eta = |E_y|/|E_x|$ and ϕ is the phase angle between the x and y components of the wave and the time dependence is

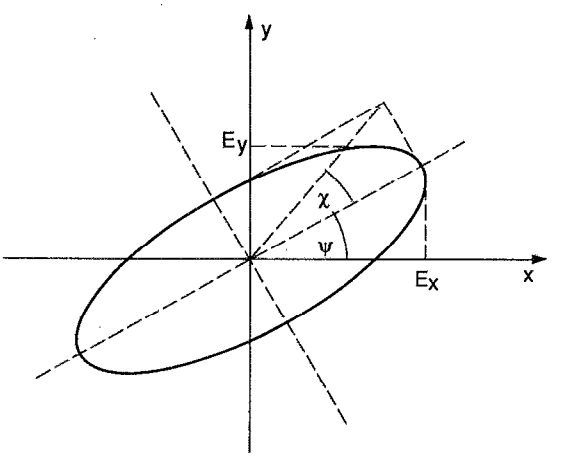

FIG. 1. Schematic diagram of the rotational ellipse showing rotation and ellipticity and the component amplitudes E_x and E_y.

ignored. The parameters η and ϕ are related to the tilt ψ of the vibrational ellipse and the ellipticity χ by (see Fig. 1)

$$\tan 2\psi = \tan 2\eta \cos \phi,$$

$$\sin 2\chi = \sin 2\eta \sin \phi.$$

The plasma birefringence (Cotton–Mouton effect) is often negligible. Later it will be convenient to ignore this effect, allowing us to set $\phi=0$ and identify $\eta=\psi$.

The first element of the polarimeter is a quarter-wave retarding optic (reflecting or transmitting) aligned so that the initial electric vector is parallel to one of the principal axes. Its Jones matrix is

$$\mathbf{Q}_0 = \begin{pmatrix} 1 & 0 \\ 0 & j \end{pmatrix}. \tag{3}$$

This is followed by an ideal analyzer (wire grid analyzer) whose matrix in transmission is

$$\mathbf{P}_\alpha^T = \begin{pmatrix} \sin^2 \alpha & -\sin \alpha \cos \alpha \\ -\sin \alpha \cos \alpha & \cos^2 \alpha \end{pmatrix} \tag{4}$$

and in reflection $\mathbf{P}_\alpha^R = -\mathbf{P}_{\alpha-\pi/2}^T$, where α is the wire orientation. For the polarimeter, the analyzer is oriented at $\alpha=45°$. In passing, note that a general polarizing reflecting element can be constructed from parallel closely spaced orthogonal polarizers (or polarizer and backing mirror) whose separation is adjustable. The matrix for such an element is $\mathbf{C}_\alpha(\delta) = \mathbf{P}_\alpha^R - \exp(j\delta)\mathbf{P}_\alpha^T$, where δ is the phase difference due to the polarizer separation. The quarter-wave plate is equivalent to $\mathbf{Q}_0 = \mathbf{C}_0(\pi/2)$.

It is readily shown that the phase shift between the radiation transmitted and reflected by the analyzer is twice the angle η (approximately equal to the Faraday angle ψ when the linear birefringence induced phase ϕ is small). The cosine of this angle is measured by mixing the waves on a square-law detector following a second analyzer oriented at 0° to maximize the interference between the orthogonally polarized components. Since η is generally small, however, it is the quadrature component that is most useful. This can also be measured interferometrically by introducing an additional quarter-wave phase shift between the orthogonal components (as in standard scintillation interferometry[13]). This additional phase shift is most conveniently obtained by replacing the first analyzer by a quarter-wave plate. The resulting layout is shown schematically in Fig. 2.

For general phase delays δ_1 and δ_2 at the phase retarding elements PR1 and PR2, the electric field of the wave reflected by the final analyzer is given by

$$\mathbf{E}_R = \mathbf{P}_0^R \mathbf{C}_{45}(\delta_2)\mathbf{C}_0(\delta_1)\mathbf{E} \tag{5}$$

and the associated intensities for both reflected and transmitted waves are

$$2I_{R,T} = 1 \pm \cos 2\eta \cos \delta_2 \pm \sin 2\eta \sin \delta_2 \sin(\phi + \delta_1). \tag{6}$$

For $\delta_2=0$ the ac component of the signals is $\pm\cos 2\eta$ as noted above. Ignoring the plasma linear birefringence and setting the delays $\delta_1=\delta_2=\pi/2$ we obtain antiphase time varying quadrature signals $\pm\sin 2\psi \approx 2\psi$. If common mode effects are insignificant an enhancement in signal to noise ratio can be obtained by subtracting the detector outputs in a differential amplifier. When laser power variations or refractive beam bending are important, however, a suitable quadrature configuration may be more appropriate.

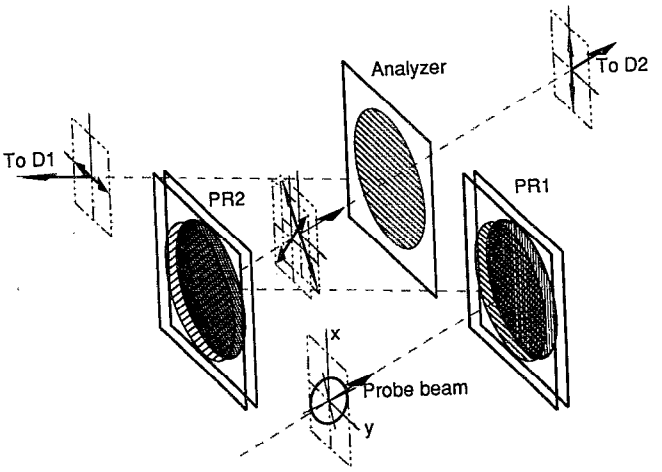

FIG. 2. Schematic diagram of the optical arrangement required for polarization analysis of the plasma probe beam. D1 and D2 are the detectors and PR1 and PR2 are polarizing reflectors.

The implementation shown in Fig. 2 could of course be replaced by crystal quarter-wave plates and a grid polarizer with certain mechanical and optical advantages. However, note that the reflecting component offers a means for sensitivity calibration by applying a small modulation $\delta_2 = \pi/2 + \epsilon(t)$ to the second polarizing reflector to obtain signals $\pm\sin(2\eta - \epsilon) \approx \pm(2\eta - \epsilon)$.

III. EXPERIMENT

A benchtop experiment constructed to test the configuration of Fig. 2 is shown schematically in Fig. 3. The source is a 150 GHz carcinotron delivering approximately 120 mW in the vertical polarization (here taken as the x axis). The beam is propagated quasioptically and focused onto a polarizing reflector $\mathbf{C}_{45}(\pi/2)$. A small sinusoidal modulation of amplitude ϵ_m is applied by mechanically vibrating the backing mirror. The resulting polarization is $\phi = -\pi/2$ and $2\eta = \epsilon_m \cos(2\pi f_m t)$ with $f_m < 1$ kHz. We thus set $\delta_1 = \pi$ and $\delta_2 = \pi/2$ to obtain detector signals proportional to 2η.

The modulation amplitude ϵ_m is monitored using a He-Ne laser Michelson interferometer ($\lambda_0 = 632.8$ nm). The number of calibration fringes F gives the total mirror translation. This is related to the phase excursion by $\epsilon_m = \lambda_0 F/(2\lambda \cos \theta)$, where $\theta = 10°$ is the angle between the He-Ne and carcinotron beams on the modulating element. A single calibration fringe is thus equivalent to a change in 2η of 0.05°.

Figure 4 shows the He-Ne interferometer fringes (top), signals from D1 and D2 (following ~55 dB amplification, 1 MHz bandwidth) (center), and the difference signal (bottom) for a modulation frequency $f_m = 130$ Hz. The p-p change in the equivalent Faraday rotation angle is $\Delta\psi \approx 0.35°$. The rms noise level is 0.35 V compared with a p-p difference signal

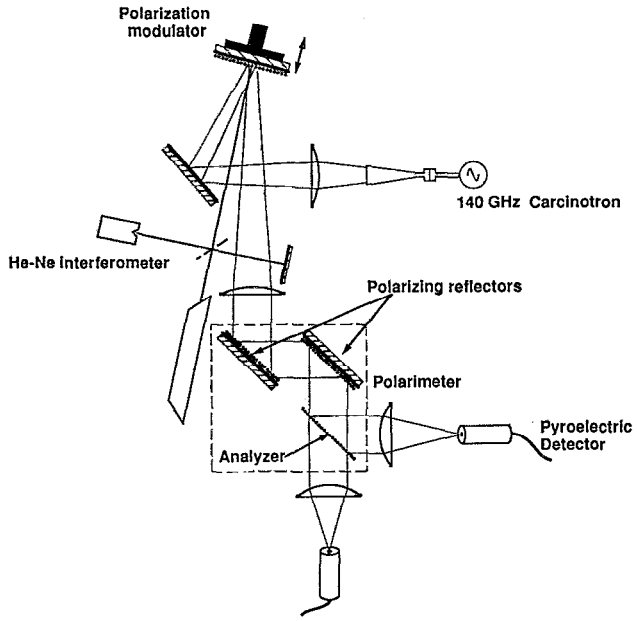

FIG. 3. Layout for the benchtop experiment designed to test the scintillation polarimeter performance. The orientations of the various polarizing components are described in the text.

excursion $\Delta S \approx 9.5$ V. After traversing the optical system, approximately 25 mW of power reaches each of the room-temperature pyroelectric detectors D1 and D2. The detector area is $A_d = \pi$ sq mm so that for the computed beam radius of 1.3 mm ($1/e$ of power profile) at the detector, about 45%

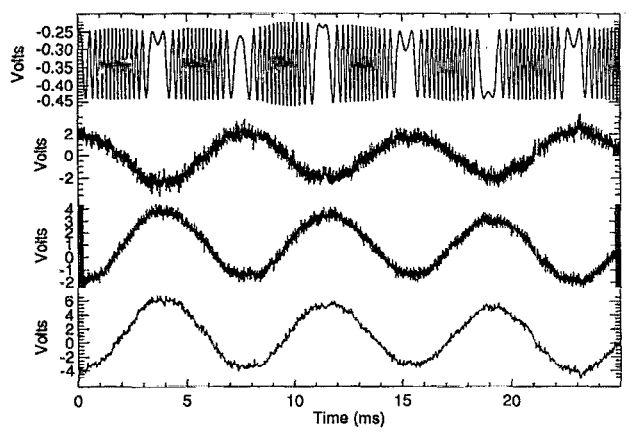

FIG. 4. He-Ne interferometer signal (top), the amplified pyroelectric detector signals (center), and their direct difference (bottom) for an equivalent Faraday rotation angle of $\psi \approx 0.35°$.

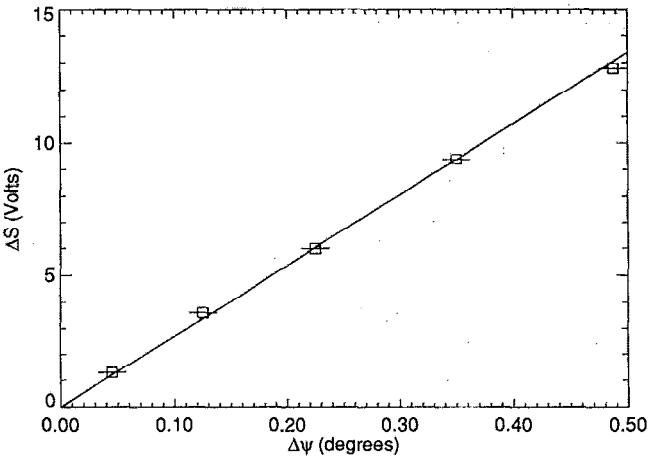

FIG. 5. Plot showing experimental confirmation of the linear relationship between the p-p difference signal level ΔS and the effective Faraday rotation angle $\Delta\psi$.

of the incident power is intercepted. The solid angle of the focused beam at the detector $\Omega \sim 0.3$ sr implies that the system etendue $A_d\Omega = 0.9$ mm^2 falls somewhat short of the maximum etendue $\sim\lambda^2 = 4.8$ mm^2.

The plot of ΔS vs $\Delta\psi$ shown in Fig. 5 exhibits the expected linearity for small angles. For low-power plasma conditions in H-1 $\bar{n}_e = 5\times10^{12}$ cm^{-3} and $B_\parallel \sim 0.1$ T the expected phase shift per pass at 150 GHz is about seven degrees. For the present system, this should be measurable with S/N ratios in excess of 500.

ACKNOWLEDGMENTS

The author wishes to thank the Australian Research Council for financial support and S. M. Hamberger for provision of the necessary facilities. The work was in part funded by grants from the Australian Institute of Nuclear Science and Engineering.

[1] F. DeMarco and S. E. Segre, Plasma Phys. **14**, 245 (1972).
[2] S. E. Segre, Plasma Phys. **20**, 295 (1978).
[3] H. J. Gardner and J. Howard, Plasma Phys. Control Fusion **36**, 245 (1994).
[4] D. Veron, in *Infrared and Millimeter Waves*, edited by K. Button (Academic, New York, 1979), Vol. 2, pp. 69–135.
[5] F. C. Jobes and D. K. Mansfield, Rev. Sci. Instrum. **63**, 5156 (1992).
[6] J. Howard, Infrared Phys. **34**, 175 (1993).
[7] H. Soltwisch, Infrared Phys. **21**, 287 (1981).
[8] G. Dodel and W. Kunz, Infrared Phys. **18**, 773 (1978).
[9] W. Kunz and G. Dodel, Plasma Phys. **20**, 171 (1978).
[10] R. Erickson, P. Forman, and F. Jahoda, IEEE Trans. Plasma Sci. **AP-17**, 275 (1984).
[11] B. W. Rice, Rev. Sci. Instrum. **63**, 5002 (1992).
[12] S. Hamberger, B. Blackwell, L. Sharp, and D. Shenton, Fusion Technol. **17**, 123 (1990).
[13] L. Sharp, Plasma Phys. **25**, 781 (1983).